Adv. Radio Sci., 23, 1–12, 2025
https://doi.org/10.5194/ars-23-1-2025


Advances in Radio Science
Open Access Proceedings

# Spherical-Multipole Analysis of the Scalar Diffraction by a Circular Aperture in a Plane Screen

**Ludger Klinkenbusch**

Department of Electrical and Information Engineering, Kiel University, Kaiserstr. 2, 24143 Kiel, Germany

**Correspondence:** Ludger Klinkenbusch (klinkenbusch@tf.uni-kiel.de)

Received: 24 January 2025 – Accepted: 24 February 2025 – Published: 14 March 2025

**Abstract.** The paper deals with a new spherical-multipole solution for the scattering of an arbitrary incident wave by a circular aperture in an acoustically soft or hard plane. The boundary-value problem is formulated as a three-domain problem. In each of the domains the field is expanded by means of a complete spherical-multipole expansion, which automatically satisfies the soft or hard boundary condition on the plane, if applicable. The multipole amplitudes of the incident field in the presence of the soft or hard plane are supposed to be given and explicitly derived for a plane wave and for a uniform Complex-Source Beam (CSB). The unknown multipole amplitudes are found from the conditions of continuity of the field and its normal derivative at the boundaries between the domains, leading to a quadratic system of linear equations. All coupling integrals are solved completely analytically. Possible and expected zeros and singularities of the field values or their derivatives at the rim of the aperture develop in the course of an increasing number of multipoles, while at the other locations a finite number of multipoles is sufficient to represent the field. The numerical evaluation validates and improves numerical results found in the literature for the geometrically complementary case of acoustically hard and soft circular discs. Further numerical results for the near- and far field exemplarily prove the robustness and convergence of the proposed method.

## 1 Introduction

Scattering and diffraction by a circular aperture in an infinitely thin impenetrable screen as shown in Fig. 1 is one of the classical canonical problems in acoustics and electromagnetics. The interest in this structure stems from both, theoretical and practical reasons. Examples for the latter are the wave coupling between hollow wave guides in microwave engineering and the analysis of the influence of apertures in EMC shielding structures, among others. From the theoretical side this structure contains a geometrical singularity at the rim of the aperture which usually implies a certain singularity of the field. Moreover, the scattering problem is a favourite example for the application of Babinet's principle, i.e., meaning that the scattered field in the region "behind" the circular aperture ($y < 0$ in Fig. 1) of radius $r_0$ in an acoustically soft (hard) plane is identical to the scattered field behind a circular disc of same radius $r_0$ consisting of an acoustically hard (soft) material. For the disc, exact analytic solutions of the corresponding acoustic boundary-value problems can be found by solving the Helmholtz equation in oblate spheroidal coordinates where the disc is one of the coordinate surfaces. Probably because of this principle and because of the finiteness of the corresponding problem, many of the solutions and numerical results found in the literature are derived for the circular disc and then adapted to the circular aperture.

Among the chronologically first attempts for a solution of an "electric" wave incident upon a circular aperture was the one presented by Rayleigh (1897). Much later Bowkamp (1941) exactly solved the disc problem analytically using spheroidal wave functions and also presented first numerical results. Bethe (1944) published a work on the diffraction by small holes and applied it to the directive coupling between wave guides (Bethe coupler) in microwave engineering. An insightful discussion of the field singularities at geometrical singularities like an edge or – as in the current case – a sharp rim including a discussion of the work by Bethe (1944) has been contributed again by Bouwkamp (1946). A direct solution of the scalar aperture problem via an integral equation formulation and a corresponding variational solution for the circular aperture in an infinite screen has been derived and

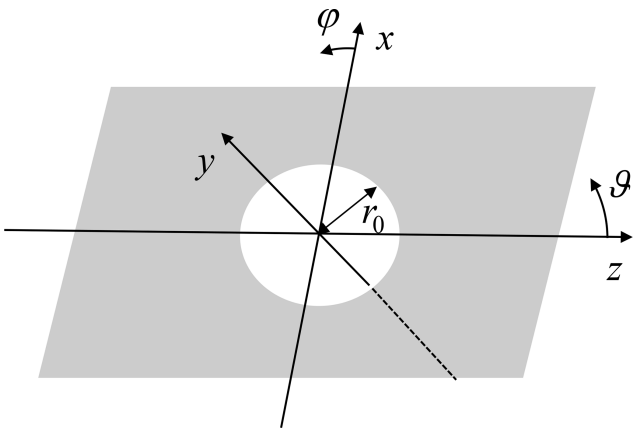


**Figure 1.** Circular aperture in a plane screen at $y = 0$.

presented in Levine and Schwinger (1948a) and Levine and Schwinger (1948b). Numerical results have been successfully compared to those ones given by Bowkamp (1941). The works by Meixner (1948) and Andrejewski (1953) solved the vector (electromagnetic) disc and aperture problem, respectively, emphasizing the role of the singularities for the unique solution of the boundary-value problem. The Meixner's edge condition states that the solution must include a certain type (degree) of singularity at the rim. Actually, while expanding the field by means of an infinite series solution which not explicitly contains this singularity, it must be developing term-by-term such that the correct singularity would be obtained only for an infinite number of terms. Braunbek (1950) applied an asymptotic method to the problem of an acoustically hard disc illuminated by a plane wave and showed that the method works fine for an surprisingly wide frequency range. De Hoop (1954) successfully investigated an approximate result derived by Bowkamp (1941). An aperture in an infinitely thin screen is also an excellent object to investigate the ability of high-frequency asymptotic methods, as has been shown in Keller (1957) and Keller et al. (1957), where the Geometrical Theory of Diffraction has been applied and tested to find an approximate solution. In Kristenssen and Waterman (1982) the exact solution using oblate spheroidal coordinates for the scalar disc problem was combined with the T-matrix method to make the disc and the aperture solutions accessible as part of more complex problems. Recently in Kurykiak and Lysechko (2015) the soft disc problem has been treated as a three-domain problem, where the analytically obtained final system of linear equations has been solved using an appropriate regularization approach.

The present paper deals with a new analytical approach to directly tackle the aperture problem. To this end, a three-domain boundary-value is formulated and corresponding spherical-multipole expansion have been formulated for both, an aperture in an acoustically soft or hard plane. The boundary-conditions are automatically satisfied by the chosen spherical-multipole functions. The unknown multipole amplitudes are found by enforcing the continuity of both, the wave functions and their derivatives. Finally a system of linear equations is obtained leading to convergent and consistent field solutions. Since the multipole expansions describing the field in the aperture do not explicitly contain any singularity or any zero field at the rim of the aperture, such a behaviour must be achieved while increasing the number of multipole amplitudes. The numerical evaluation includes a convergence analysis, a validation and several results for a plane wave as well as a uniform complex-source beam, each incident on a circular aperture in an acoustically soft and in an acoustically hard infinite screen. Besides the solution of a coupling integral with a product of two Ferrers functions with different degrees and orders, the appendix includes the derivation of the multipole amplitudes for an arbitrary incident plane wave and for a uniform complex-source beam, each in the presence of an acoustically soft or hard plane.

Parts of this work have been presented at conferences, see Klinkenbusch (2024a, b). A study on the corresponding 2D case (for the slit) has been published in Klinkenbusch (2019).

## 2 Formulation of the three-dimensional boundary-value problem

Consider a circular aperture in an infinitely extended acoustically soft or hard plane as sketched in Fig. 1. In Cartesian coordinates the plane is described by $y = 0$ while the circular aperture of radius $r_0$ is symmetrically located around the origin. We introduce spherical coordinates $r, \vartheta, \varphi$ according to $x = r\sin\vartheta\cos\varphi$, $y = r\sin\vartheta\sin\varphi$, $z = r\cos\vartheta$ and split the entire space into three domains as shown in Fig. 2, with total fields $\psi^{\mathrm{I}}, \psi^{\mathrm{II}}, \psi^{\mathrm{III}}$ in each domain. Domain I and II are defined by $r > r_0$, $y > 0$ and $r > r_0$, $y < 0$, respectively. Domain III consists of a sphere with radius $r_0$ centered at the origin and thus includes the entire aperture. In domain I we split the total field into a given incident ($\psi^{\mathrm{inc}}$) and into a scattered ($\psi^{\mathrm{sca}}$) part. The other domains are supposed to be source-free. In the following, we are seeking for time-harmonic solutions of the Helmholtz equation described by phasors at a time factor $e^{+j\omega t}$. We derive exact spherical-multipole expansions of the fields everywhere and for both cases, i.e., a circular aperture in a soft (index s) and in a hard (index h) infinite plane with $\psi_{\mathrm{s}}^{\mathrm{I}}|_{y=0} = \psi_{\mathrm{s}}^{\mathrm{II}}|_{y=0} = 0$ and $\partial\psi_{\mathrm{h}}^{\mathrm{I}}/\partial\varphi|_{y=0} = \partial\psi_{\mathrm{h}}^{\mathrm{II}}/\partial\varphi|_{y=0} = 0$, respectively.

## 3 Solution of the boundary-value problem for a circular aperture in an acoustically soft plane

In each of the domains I, II we introduce a complete spherical-multipole expansion for the total field satisfying the boundary condition imposed by the acoustically soft plane, while the total field in domain III is developed by

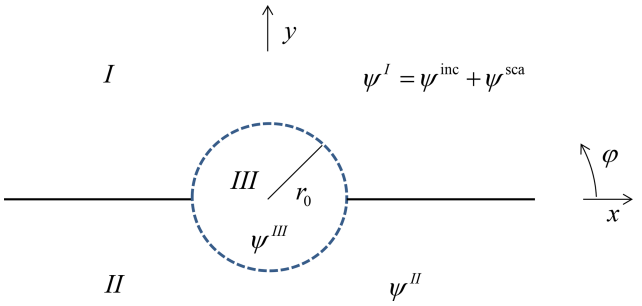


**Figure 2.** Definition of the three domains.

means of a general spherical-multipole expansion

$$\psi_s^{\mathrm{I}}(r,\vartheta,\varphi) = \sum_{n=1}^{n^{\mathrm{inc}}}\sum_{m=1}^{n} a_{nm}^{\mathrm{inc}} j_n(\kappa r) Y_{nm}^{(\mathrm{o})}(\vartheta,\varphi) + \sum_{n=1}^{n^{\mathrm{sca}}}\sum_{m=1}^{n} a_{nm}^{\mathrm{sca}} h_n^{(2)}(\kappa r) Y_{nm}^{(\mathrm{o})}(\vartheta,\varphi) \quad (1)$$

$$\psi_s^{\mathrm{II}}(r,\vartheta,\varphi) = \sum_{n=1}^{n^{\mathrm{sca}}}\sum_{m=1}^{n} a_{nm}^{\mathrm{II}} h_n^{(2)}(\kappa r) Y_{nm}^{(\mathrm{o})}(\vartheta,\varphi) \quad (2)$$

$$\psi_s^{\mathrm{III}}(r,\vartheta,\varphi) = \sum_{n=1}^{n^{\mathrm{III}}}\sum_{m=1}^{n} a_{nm}^{\mathrm{III}} j_n(\kappa r) Y_{nm}^{(\mathrm{o})}(\vartheta,\varphi) + \sum_{n=0}^{n^{\mathrm{III}}}\sum_{m=0}^{n} b_{nm}^{\mathrm{III}} j_n(\kappa r) Y_{nm}^{(\mathrm{e})}(\vartheta,\varphi). \quad (3)$$

Note that in addition in domain I the field is splitted into a (known) incident and a scattered part, each satisfying the boundary condition on the plane. In Eqs. (1)–(3), $j_n$ and $h_n^{(2)}$ represent spherical Bessel functions of the first kind and spherical Hankel functions of the second kind, to guarantee regularity everywhere and to comply with the Sommerfeld radiation condition, respectively. For an exact solution the upper limits of the sums in Eqs. (1)–(3), $n^{\mathrm{inc}}, n^{\mathrm{sca}}$, and $n^{\mathrm{III}}$, in general each have to become infinitely large. The normalized odd [index (o)] and even [index (e)] surface-spherical harmonics are defined by

$$Y_{nm}^{(\mathrm{o})}(\vartheta,\varphi) = \sqrt{\frac{2n+1}{2\pi}\frac{(n-m)!}{(n+m)!}} P_n^m(\cos\vartheta)\sin(m\varphi) \quad (4)$$

$$Y_{nm}^{(\mathrm{e})}(\vartheta,\varphi) = \sqrt{\frac{2n+1}{2\pi\epsilon_m}\frac{(n-m)!}{(n+m)!}} P_n^m(\cos\vartheta)\cos(m\varphi) \quad (5)$$

where $P_n^m$ denotes a Ferrers' function, i.e., an associated Legendre function of the first kind "on the cut", see DLMF (2024), and where the Neumann number is given by $\epsilon_m = 2$ if $m = 0$ and $\epsilon_m = 1$ if $m = 1, 2, 3, \ldots$. On a closed spherical surface the surface spherical harmonics form a complete orthonormalized system for any solution of the Helmholtz operator according to

$$\int_0^{\pi}\int_0^{2\pi} Y_{nm}^{(\mathrm{o})}(\vartheta,\varphi) Y_{n'm'}^{(\mathrm{o})}(\vartheta,\varphi)\sin\vartheta\,\mathrm{d}\vartheta\,\mathrm{d}\varphi = \delta_{nn'}\delta_{mm'} \quad (6)$$

$$\int_0^{\pi}\int_0^{2\pi} Y_{nm}^{(\mathrm{e})}(\vartheta,\varphi) Y_{n'm'}^{(\mathrm{e})}(\vartheta,\varphi)\sin\vartheta\,\mathrm{d}\vartheta\,\mathrm{d}\varphi = \delta_{nn'}\delta_{mm'} \quad (7)$$

$$\int_0^{\pi}\int_0^{2\pi} Y_{nm}^{(\mathrm{o})}(\vartheta,\varphi) Y_{n'm'}^{(\mathrm{e})}(\vartheta,\varphi)\sin\vartheta\,\mathrm{d}\vartheta\,\mathrm{d}\varphi = 0 \quad (8)$$

$$\sum_{n=0}^{\infty}\sum_{m=0}^{n}\left[Y_{nm}^{(\mathrm{o})}(\vartheta,\varphi) Y_{nm}^{(\mathrm{o})}(\vartheta',\varphi') + Y_{nm}^{(\mathrm{e})}(\vartheta,\varphi) Y_{nm}^{(\mathrm{e})}(\vartheta',\varphi')\right] \widehat{=} \frac{\delta(\vartheta-\vartheta')\delta(\varphi-\varphi')}{\sin\vartheta} \quad (9)$$

with the Dirac $\delta$-functional $\delta(x)$ and the Kronecker symbol defined by $\delta_{ij} = 1$ if $i = j$ and $\delta_{ij} = 0$ if $i \neq j$. Since (throughout the paper) an arbitrary incident field in domain I in defined as the field in the presence of the acoustically soft plane at $y = 0$, it includes the reflected field and differs from the classical definition of the incident field in scattering problems. We anticipate that the multipole amplitudes of such an incident field are known, examples are represented in Appendix B and C. For the determination of all other multipole coefficients we have to consider the boundary- and continuity conditions. In particular, at the boundary at $r = r_0$, the total fields as well as their normal derivatives have to be continuous

$$\psi_s^{\mathrm{III}}\big|_{r=r_0} = \begin{cases} \psi_s^{\mathrm{I}}\big|_{r=r_0} & 0<\vartheta<\pi; 0<\varphi<\pi \\ \psi_s^{\mathrm{II}}\big|_{r=r_0} & 0<\vartheta<\pi; \pi<\varphi<2\pi \end{cases} \quad (10)$$

$$\left.\frac{\partial\psi_s^{\mathrm{III}}}{\partial r}\right|_{r=r_0} = \begin{cases} \left.\frac{\partial\psi_s^{\mathrm{I}}}{\partial r}\right|_{r=r_0} & 0<\vartheta<\pi; 0<\varphi<\pi \\ \left.\frac{\partial\psi_s^{\mathrm{II}}}{\partial r}\right|_{r=r_0} & 0<\vartheta<\pi; \pi<\varphi<2\pi. \end{cases} \quad (11)$$

We insert Eqs. (1)–(3) into Eq. (10), multiply the result by $Y_{n'm'}^{(\mathrm{o})}\sin\vartheta$, integrate on the interval $0<\vartheta<\pi; 0<\varphi<2\pi$, and finally obtain because of the orthogonality relations Eqs. (6)–(8)

$$\begin{aligned} a_{nm}^{\mathrm{III}} j_n(\kappa r_0) = &\sum_{n'=1}^{n^{\mathrm{inc}}}\sum_{m'=1}^{n'} a_{n'm'}^{\mathrm{inc}} j_{n'}(\kappa r_0) < Y_{n'm'}^{(\mathrm{o})}, Y_{nm}^{(\mathrm{o})} >_1 \\ &+ \sum_{n'=1}^{n^{\mathrm{sca}}}\sum_{m'=1}^{n'} a_{n'm'}^{\mathrm{sca}} h_{n'}^{(2)}(\kappa r_0) < Y_{n'm'}^{(\mathrm{o})}, Y_{nm}^{(\mathrm{o})} >_1 \\ &+ \sum_{n'=1}^{n^{\mathrm{sca}}}\sum_{m'=1}^{n'} a_{n'm'}^{\mathrm{II}} h_{n'}^{(2)}(\kappa r_0) < Y_{n'm'}^{(\mathrm{o})}, Y_{nm}^{(\mathrm{o})} >_2 \\ &(n = 1, 2, \ldots, n^{\mathrm{III}}; m = 1, 2, \ldots, n). \end{aligned} \quad (12)$$

In Eq. (12) and in the following the scalar products are defined according to

$$< Y_{nm}, Y_{n'm'} >_1 = \int_{\vartheta=0}^{\pi} \int_{\varphi=0}^{\pi} Y_{nm} Y_{n'm'} \sin\vartheta \, \mathrm{d}\vartheta \, \mathrm{d}\varphi \tag{13}$$

$$< Y_{nm}, Y_{n'm'} >_2 = \int_{\vartheta=0}^{\pi} \int_{\varphi=\pi}^{2\pi} Y_{nm} Y_{n'm'} \sin\vartheta \, \mathrm{d}\vartheta \, \mathrm{d}\varphi. \tag{14}$$

Next, multiplying Eq. (10) by $Y^{(\mathrm{e})}_{n'm'} \sin\vartheta$ and integrating on $0 < \vartheta < \pi; 0 < \varphi < 2\pi$ leads to

$$\begin{aligned} b^{\mathrm{III}}_{nm} j_n(\kappa r_0) = & \sum_{n'=1}^{n^{\mathrm{inc}}} \sum_{m'=1}^{n'} a^{\mathrm{inc}}_{n'm'} j_{n'}(\kappa r_0) < Y^{(\mathrm{o})}_{n'm'}, Y^{(\mathrm{e})}_{nm} >_1 \\ & + \sum_{n'=1}^{n^{\mathrm{sca}}} \sum_{m'=1}^{n'} a^{\mathrm{sca}}_{n'm'} h^{(2)}_{n'}(\kappa r_0) < Y^{(\mathrm{o})}_{n'm'}, Y^{(\mathrm{e})}_{nm} >_1 \\ & + \sum_{n'=1}^{n^{\mathrm{sca}}} \sum_{m'=1}^{n'} a^{\mathrm{II}}_{n'm'} h^{(2)}_{n'}(\kappa r_0) < Y^{(\mathrm{o})}_{n'm'}, Y^{(\mathrm{e})}_{nm} >_2 \\ & (n = 0, 1, 2, \ldots, n^{\mathrm{III}}; m = 0, 1, 2, \ldots, n) \end{aligned} \tag{15}$$

Correspondingly, inserting Eqs. (1)–(3) into Eq. (11) and multiplying the result subsequently by $Y^{(\mathrm{o})}_{nm} \sin\vartheta$ and by $Y^{(\mathrm{e})}_{nm} \sin\vartheta$ and each integrating on $0 < \vartheta < \pi; 0 < \varphi < 2\pi$ yields

$$\begin{aligned} & a^{\mathrm{III}}_{nm} \left. \frac{\mathrm{d} j_n(\kappa r)}{\mathrm{d}\kappa r} \right|_{r=r_0} = \sum_{n'=1}^{n^{\mathrm{inc}}} \sum_{m'=1}^{n'} a^{\mathrm{inc}}_{n'm'} \left. \frac{\mathrm{d} j_{n'}(\kappa r)}{\mathrm{d}\kappa r} \right|_{r=r_0} \\ & < Y^{(\mathrm{o})}_{n'm'}, Y^{(\mathrm{o})}_{nm} >_1 + \sum_{n'=1}^{n^{\mathrm{sca}}} \sum_{m'=1}^{n'} a^{\mathrm{sca}}_{n'm'} \left. \frac{\mathrm{d} h^{(2)}_{n'}(\kappa r)}{\mathrm{d}\kappa r} \right|_{r=r_0} \\ & < Y^{(\mathrm{o})}_{n'm'}, Y^{(\mathrm{o})}_{nm} >_1 + \sum_{n'=1}^{n^{\mathrm{sca}}} \sum_{m'=1}^{n'} a^{\mathrm{II}}_{n'm'} \left. \frac{\mathrm{d} h^{(2)}_{n'}(\kappa r)}{\mathrm{d}\kappa r} \right|_{r=r_0} \\ & < Y^{(\mathrm{o})}_{n'm'}, Y^{(\mathrm{o})}_{nm} >_2 \quad (n = 1, 2, \ldots, n^{\mathrm{III}}; m = 1, 2, \ldots, n) \end{aligned} \tag{16}$$

and

$$\begin{aligned} & b^{\mathrm{III}}_{nm} \left. \frac{\mathrm{d} j_n(\kappa r)}{\mathrm{d}\kappa r} \right|_{r=r_0} = \sum_{n'=1}^{n^{\mathrm{inc}}} \sum_{m'=1}^{n'} a^{\mathrm{inc}}_{n'm'} \left. \frac{\mathrm{d} j_{n'}(\kappa r)}{\mathrm{d}\kappa r} \right|_{r=r_0} \\ & < Y^{(\mathrm{o})}_{n'm'}, Y^{(\mathrm{e})}_{nm} >_1 + \sum_{n'=1}^{n^{\mathrm{sca}}} \sum_{m'=1}^{n'} a^{\mathrm{sca}}_{n'm'} \left. \frac{\mathrm{d} h^{(2)}_{n'}(\kappa r)}{\mathrm{d}\kappa r} \right|_{r=r_0} \\ & < Y^{(\mathrm{o})}_{n'm'}, Y^{(\mathrm{e})}_{nm} >_1 + \sum_{n'=1}^{n^{\mathrm{sca}}} \sum_{m'=1}^{n'} a^{\mathrm{II}}_{n'm'} \left. \frac{\mathrm{d} h^{(2)}_{n'}(\kappa r)}{\mathrm{d}\kappa r} \right|_{r=r_0} \\ & < Y^{(\mathrm{o})}_{n'm'}, Y^{(\mathrm{e})}_{nm} >_2 (n = 0, 1, 2, \ldots, n^{\mathrm{III}}; m = 0, 1, 2, \ldots, n), \end{aligned} \tag{17}$$

respectively. As easily can be shown it holds

$$< Y^{(\mathrm{o})}_{n'm'}, Y^{(\mathrm{o})}_{nm} >_1 = < Y^{(\mathrm{o})}_{n'm'}, Y^{(\mathrm{o})}_{nm} >_2 = \frac{1}{2} \delta_{n,n'} \delta_{m,m'}. \tag{18}$$

Hence it follows from Eqs. (12) and (16) that

$$\begin{aligned} a^{\mathrm{III}}_{nm} j_n(\kappa r_0) = & \frac{1}{2} \Big[ a^{\mathrm{inc}}_{nm} j_n(\kappa r_0) + a^{\mathrm{sca}}_{nm} h^{(2)}_n(\kappa r_0) \\ & + a^{\mathrm{II}}_{nm} h^{(2)}_n(\kappa r_0) \Big] \quad (n = 1, 2, \ldots; m = 1, 2, \ldots, n) \end{aligned} \tag{19}$$

and

$$\begin{aligned} a^{\mathrm{III}}_{nm} \left. \frac{\mathrm{d} j_n(\kappa r)}{\mathrm{d}\kappa r} \right|_{r=r_0} = & \frac{1}{2} \left[ a^{\mathrm{inc}}_{nm} \left. \frac{\mathrm{d} j_n(\kappa r)}{\mathrm{d}\kappa r} \right|_{r=r_0} \right. \\ & \left. + a^{\mathrm{sca}}_{nm} \left. \frac{\mathrm{d} h^{(2)}_n(\kappa r)}{\mathrm{d}\kappa r} \right|_{r=r_0} + a^{\mathrm{II}}_{nm} \left. \frac{\mathrm{d} h^{(2)}_n(\kappa r)}{\mathrm{d}\kappa r} \right|_{r=r_0} \right] \\ & (n = 1, 2, \ldots; m = 1, 2, \ldots, n) \end{aligned} \tag{20}$$

We multiply Eq. (19) by $\left. \frac{\mathrm{d} j_n(\kappa r)}{\mathrm{d}\kappa r} \right|_{r=r_0}$ and subtract from the results the product of Eq. (20) and $j_n(\kappa r_0)$

$$\begin{aligned} & \frac{1}{2} \left[ a^{\mathrm{sca}}_{nm} + a^{\mathrm{II}}_{nm} \right] \left[ h^{(2)}_n(\kappa r_0) \left. \frac{\mathrm{d} j_n(\kappa r)}{\mathrm{d}\kappa r} \right|_{r=r_0} \right. \\ & \left. - \left. \frac{\mathrm{d} h^{(2)}_n(\kappa r)}{\mathrm{d}\kappa r} \right|_{r=r_0} j_n(\kappa r_0) \right] = 0. \end{aligned} \tag{21}$$

Because the Wronski determinant of a fundamental system has no zeroes we conclude from Eq. (21)

$$a^{\mathrm{sca}}_{nm} = -a^{\mathrm{II}}_{nm}, \tag{22}$$

which reflects the symmetry of the scattered fields (according to the current definition of the incident field which includes the reflected field) with respect to the plane $y = 0$. Moreover, with Eq. (22) we immediately derive from Eq. (19)

$$a^{\mathrm{III}}_{nm} = \frac{1}{2} a^{\mathrm{inc}}_{nm}. \tag{23}$$

As can be easily shown it holds

$$\begin{aligned} & < Y^{(\mathrm{o})}_{n'm'}, Y^{(\mathrm{e})}_{nm} >_1 = - < Y^{(\mathrm{o})}_{n'm'}, Y^{(\mathrm{e})}_{nm} >_2 \\ & = N_{nm,n'm'} \int_{-1}^{1} P^m_n(x) P^{m'}_{n'}(x) \mathrm{d}x \begin{cases} \frac{2m'}{m'^2 - m^2} & \begin{matrix} m'-m \\ n'-n \end{matrix} \text{odd} \\ 0 & \text{else,} \end{cases} . \end{aligned} \tag{24}$$

where the normalization constant is given by

$$N_{nm,n'm'} = \sqrt{\frac{(2n+1)(2n'+1)}{4\pi^2 \epsilon_m} \frac{(n-m)!(n'-m')!}{(n+m)!(n'+m')!}}. \tag{25}$$

Moreover, the remaining integral in Eq. (24) can also be analytically solved in a closed form. As shown in Appendix A

it holds

$$\int_{-1}^{+1} P_n^m(x)\,P_{n'}^{m'}(x)\mathrm{d}x = \begin{cases} \sum_{p=0}^{p_{\max}}\sum_{p'=0}^{p'_{\max}} \alpha_{n,m}^{p}\alpha_{n',m'}^{p'} \\ \frac{\Gamma\left[\frac{1}{2}(n-n'-m-m'-2p-2p'+1)\right]\Gamma\left[\frac{1}{2}(m+m'+2p+2p'+2)\right]}{\Gamma\left[\frac{1}{2}(n+n'+3)\right]} \\ \qquad n+m+n'+m' \ \text{ even} \\ 0 \qquad \text{else,} \end{cases} \tag{26}$$

where $\Gamma(x)$ represents the Gamma function and where

$$\alpha_{n,m}^{p} = \frac{(-1)^{p+m}(n+m)!}{2^{m+2p}(m+p)!p!(n-m-2p)!}, \tag{27}$$

$$p_{\max} = \lfloor\frac{n-m}{2}\rfloor \qquad p'_{\max} = \lfloor\frac{n'-m'}{2}\rfloor. \tag{28}$$

In Eq. (28), $\lfloor x\rfloor$ represents the largest integer $\leq x$. Now multiplying Eq. (15) by $\frac{\mathrm{d}j_{n'}(\kappa r_0)}{\mathrm{d}\kappa r_0}$ and subtracting from the result the product of Eq. (17) and $j_{n'}(\kappa r_0)$ we derive with Eq. (22) and Eq. (24)

$$\begin{aligned} &2\sum_{\substack{n=1\\ n-n' \text{ odd}}}^{n^{\mathrm{sca}}}\sum_{\substack{m=1\\ m-m' \text{ odd}}}^{n} a_{nm}^{\mathrm{sca}} < Y_{nm}^{(\mathrm{o})}, Y_{n'm'}^{(\mathrm{e})} >_1 \\ &\quad\left[\frac{\mathrm{d}j_{n'}(\kappa r_0)}{\mathrm{d}\kappa r_0}h_n^{(2)}(\kappa r_0) - j_{n'}(\kappa r_0)\frac{\mathrm{d}h_n^{(2)}(\kappa r_0)}{\mathrm{d}\kappa r_0}\right] \\ &= -\sum_{\substack{n=1\\ n-n' \text{ odd}}}^{n^{\mathrm{inc}}}\sum_{\substack{m=1\\ m-m' \text{ odd}}}^{n} a_{nm}^{\mathrm{inc}} < Y_{nm}^{(\mathrm{o})}, Y_{n'm'}^{(\mathrm{e})} >_1 \\ &\quad\left[j_n(\kappa r_0)\frac{\mathrm{d}j_{n'}(\kappa r_0)}{\mathrm{d}\kappa r_0} - \frac{\mathrm{d}j_n(\kappa r_0)}{\mathrm{d}\kappa r_0}j_{n'}(\kappa r_0)\right] \\ &\quad (n'=0,1,2,\ldots,n^{\mathrm{III}}; m'=0,1,2,\ldots,n'), \end{aligned} \tag{29}$$

which can be written as a finite system of linear equations to determine the $a_{nm}^{\mathrm{sca}}$ from the $a_{nm}^{\mathrm{inc}}$

$$\begin{pmatrix} A_{00,11} & A_{00,21} & A_{00,22} & \ldots & A_{00,NN} \\ A_{10,11} & A_{10,21} & A_{10,22} & \ldots & A_{10,NN} \\ A_{11,11} & A_{11,21} & A_{11,22} & \ldots & A_{11,NN} \\ \vdots & \vdots & \vdots & \vdots & \\ A_{MM,11} & A_{MM,21} & A_{MM,22} & \ldots & A_{MM,NN} \end{pmatrix} \begin{pmatrix} a_{11}^{\mathrm{sca}} \\ a_{21}^{\mathrm{sca}} \\ a_{22}^{\mathrm{sca}} \\ \vdots \\ a_{NN}^{\mathrm{sca}} \end{pmatrix} = \begin{pmatrix} A_{00}^{\mathrm{inc}} \\ A_{10}^{\mathrm{inc}} \\ A_{11}^{\mathrm{inc}} \\ \vdots \\ A_{MM}^{\mathrm{inc}} \end{pmatrix}. \tag{30}$$

The elements of the matrix in Eq. (30) are found as

$$A_{nm,n'm'} = \begin{cases} 2 < Y_{n'm'}^{(\mathrm{o})}, Y_{nm}^{(\mathrm{e})} >_1 \\ \left[h_{n'}^{(2)}(\kappa r_0)\frac{\mathrm{d}j_n(\kappa r_0)}{\mathrm{d}\kappa r_0} - \frac{\mathrm{d}h_{n'}^{(2)}(\kappa r_0)}{\mathrm{d}\kappa r_0}j_n(\kappa r_0)\right] & \begin{matrix} n-n' \text{odd} \\ \text{and} \\ m-m' \text{odd} \end{matrix} \\ 0 \quad \text{else,} \end{cases} \tag{31}$$

while for the elements of the right-hand side we obtain

$$A_{nm}^{\mathrm{inc}} = \begin{cases} -\sum_{\substack{n'=1\\ n-n' \text{ odd}}}^{n^{\mathrm{inc}}}\sum_{\substack{m'=1\\ m-m' \text{ odd}}}^{n'} a_{n'm'}^{\mathrm{inc}} < Y_{n'm'}^{(\mathrm{o})}, Y_{nm}^{(\mathrm{e})} >_1 \\ \left[j_{n'}(\kappa r_0)\frac{\mathrm{d}j_n(\kappa r_0)}{\mathrm{d}\kappa r_0} - \frac{\mathrm{d}j_{n'}(\kappa r_0)}{\mathrm{d}\kappa r_0}j_n(\kappa r_0)\right] & \begin{matrix} n-n' \text{odd} \\ \text{and} \\ m-m' \text{odd} \end{matrix} \\ 0 \quad \text{else.} \end{cases} \tag{32}$$

For a quadratic system of linear equations in Eq. (30) we choose for the upper limits

$$N = n^{\mathrm{sca}}; \quad M = n^{\mathrm{III}} = n^{\mathrm{sca}} - 1. \tag{33}$$

Note that this kind of determination of the multipole amplitudes via a dense system of linear equations is referred to as being "non-final", see Sommerfeld (1947). A change of the maximum number of scattered-field multipoles leads to a different degree of the system of linear equations and thus potentially changes all scattered-field multipole amplitudes.

Finally, with Eq. (22) the remaining multipole amplitudes in domain III can be found from Eqs. (15) and (17) according to

$$\begin{aligned} b_{nm}^{\mathrm{III}} &= \frac{1}{j_n(\kappa r_0) + \frac{\mathrm{d}j_n(\kappa r_0)}{\mathrm{d}\kappa r_0}} \\ &\left\{ \sum_{\substack{n'=1\\ n-n' \text{ odd}}}^{n^{\mathrm{inc}}}\sum_{\substack{m'=1\\ m-m' \text{ odd}}}^{n'} a_{n'm'}^{\mathrm{inc}}\left(j_{n'}(\kappa r_0) + \frac{\mathrm{d}j_{n'}(\kappa r_0)}{\mathrm{d}\kappa r_0}\right) < Y_{n'm'}^{(\mathrm{o})}, Y_{nm}^{(\mathrm{e})} >_1 \right. \\ &+2\sum_{\substack{n'=1\\ n-n' \text{ odd}}}^{n^{\mathrm{sca}}}\sum_{\substack{m'=1\\ m-m' \text{ odd}}}^{n'} a_{n'm'}^{\mathrm{sca}}\left(h_{n'}^{(2)}(\kappa r_0) + \frac{\mathrm{d}h_{n'}^{(2)}(\kappa r_0)}{\mathrm{d}\kappa r_0}\right) < Y_{n'm'}^{(\mathrm{o})}, \\ &\left. Y_{nm}^{(\mathrm{e})} >_1 \right\} \quad (n=0,1,2,\ldots,n^{\mathrm{III}}; m=0,1,2,\ldots,n). \end{aligned} \tag{34}$$

Note that the attempt to determine the $b_{nm}^{\mathrm{III}}$ just from Eq. (15) or from Eq. (17) would be not defined for the resonance cases, i.e., for the zeros of the spherical Bessel functions or of their derivatives, respectively. Finally, using the asymptotic expression of the spherical Hankel function of the second kind for large values of its argument

$$h_n^{(2)}(\kappa r) \cong j^{n+1}\frac{e^{-j\kappa r}}{\kappa r}, \tag{35}$$

we define the far-field in domain II from Eqs. (2) and (35) dropping the spherical-wave term;

$$\psi_{\mathrm{s},\infty}^{\mathrm{II}}(r,\vartheta,\varphi) = \sum_{n=1}^{n^{\mathrm{sca}}}\sum_{m=1}^{n} j^{n+1}a_{nm}^{\mathrm{II}}Y_{nm}^{(\mathrm{o})}(\vartheta,\varphi). \tag{36}$$

## 4 Solution of the boundary-value problem for a circular aperture in an acoustically hard plane

In each of the domains I, II, and III we introduce a complete spherical-multipole expansion for the total field according to

$$\psi_{\mathrm{h}}^{\mathrm{I}}(r,\vartheta,\varphi)=\sum_{n=0}^{n^{\mathrm{inc}}}\sum_{m=0}^{n} b_{nm}^{\mathrm{inc}}\, j_n(\kappa r)\, Y_{nm}^{(\mathrm{e})}(\vartheta,\varphi) + \sum_{n=0}^{n^{\mathrm{sca}}}\sum_{m=0}^{n} b_{nm}^{\mathrm{sca}}\, h_n^{(2)}(\kappa r)\, Y_{nm}^{(\mathrm{e})}(\vartheta,\varphi) \tag{37}$$

$$\psi_{\mathrm{h}}^{\mathrm{II}}(r,\vartheta,\varphi)=\sum_{n=0}^{n^{\mathrm{sca}}}\sum_{m=0}^{n} b_{nm}^{\mathrm{II}}\, h_n^{(2)}(\kappa r)\, Y_{nm}^{(\mathrm{e})}(\vartheta,\varphi) \tag{38}$$

$$\psi_{\mathrm{h}}^{\mathrm{III}}(r,\vartheta,\varphi)=\sum_{n=1}^{n^{\mathrm{III}}}\sum_{m=1}^{n} \alpha_{nm}^{\mathrm{III}}\, j_n(\kappa r)\, Y_{nm}^{(\mathrm{o})}(\vartheta,\varphi) + \sum_{n=0}^{n^{\mathrm{III}}}\sum_{m=0}^{n} \beta_{nm}^{\mathrm{III}}\, j_n(\kappa r)\, Y_{nm}^{(\mathrm{e})}(\vartheta,\varphi). \tag{39}$$

Note that the incident field represented by the spherical multipole amplitudes $b_{nm}^{\mathrm{inc}}$ again is defined as an arbitrary incident field in domain I in the presence of the acoustically hard plane at $y=0$, i.e., it includes the reflected field and thus differs from the classical definition of an incident field in scattering problems.

The multipole amplitudes of such an incident field $b_{nm}^{\mathrm{inc}}$ are known. For the determination of the other multipole coefficients we have to consider the boundary- and continuity conditions according to Eqs. (10)–(11). A quite similar analysis as shown in Sect. 3 leads to the relations

$$b_{nm}^{\mathrm{sca}} = -b_{nm}^{\mathrm{II}} \tag{40}$$

and

$$\beta_{nm}^{\mathrm{III}} = \frac{1}{2} b_{nm}^{\mathrm{inc}}. \tag{41}$$

The multipole amplitudes of the scattered field are found from the solution of the system of linear equations

$$\begin{pmatrix} C_{11,00} & C_{11,10} & C_{11,11} & \dots & C_{11,MM} \\ C_{21,00} & C_{21,10} & C_{21,11} & \dots & C_{21,MM} \\ C_{22,00} & C_{22,10} & C_{22,11} & \dots & C_{22,MM} \\ \vdots & \vdots & \vdots & \vdots & \\ C_{NN,00} & C_{NN,10} & C_{NN,11} & \dots & C_{NN,MM} \end{pmatrix} \begin{pmatrix} b_{00}^{\mathrm{sca}} \\ b_{10}^{\mathrm{sca}} \\ b_{11}^{\mathrm{sca}} \\ \vdots \\ b_{MM}^{\mathrm{sca}} \end{pmatrix} = \begin{pmatrix} D_{11}^{\mathrm{inc}} \\ D_{21}^{\mathrm{inc}} \\ D_{22}^{\mathrm{inc}} \\ \vdots \\ D_{NN}^{\mathrm{inc}} \end{pmatrix}. \tag{42}$$

The elements of the matrix in Eq. (42) are given by

$$C_{nm,n'm'} = \begin{cases} 2 < Y_{n'm'}^{(\mathrm{e})}, Y_{nm}^{(\mathrm{o})} >_1 \times \\ \left[ h_{n'}^{(2)}(\kappa r_0) \frac{\mathrm{d}j_n(\kappa r_0)}{\mathrm{d}\kappa r_0} - \frac{\mathrm{d}h_{n'}^{(2)}(\kappa r_0)}{\mathrm{d}\kappa r_0} j_n(\kappa r_0) \right] & \begin{matrix} n-n' \text{odd} \\ \text{and} \\ m-m' \text{odd} \end{matrix} \\ 0 \quad \text{else,} \end{cases} \tag{43}$$

while for the elements of the right-hand side we obtain

$$D_{nm}^{\mathrm{inc}} = \begin{cases} -\sum_{\substack{n'=0 \\ n-n' \\ \text{odd}}}^{n^{\mathrm{inc}}} \sum_{\substack{m'=0 \\ m-m' \\ \text{odd}}}^{n'} b_{n'm'}^{\mathrm{inc}} < Y_{n'm'}^{(\mathrm{e})}, Y_{nm}^{(\mathrm{o})} >_1 \times \\ \left[ j_{n'}(\kappa r_0) \frac{\mathrm{d}j_n(\kappa r_0)}{\mathrm{d}\kappa r_0} - \frac{\mathrm{d}j_{n'}(\kappa r_0)}{\mathrm{d}\kappa r_0} j_n(\kappa r_0) \right] & \begin{matrix} n-n' \text{odd} \\ \text{and} \\ m-m' \text{odd} \end{matrix} \\ 0 \quad \text{else.} \end{cases} \tag{44}$$

For a quadratic system of linear equations in Eq. (42) we choose for the upper limits $N = n^{\mathrm{sca}}$ and $M = n^{\mathrm{III}} = n^{\mathrm{sca}} - 1$. The remaining multipole amplitudes in the domain III are then found according to

$$\alpha_{nm}^{\mathrm{III}} = \frac{1}{j_n(\kappa r_0) + \frac{\mathrm{d}j_n(\kappa r_0)}{\mathrm{d}\kappa r_0}} \left\{ \sum_{\substack{n'=0 \\ n-n' \\ \text{odd}}}^{n^{\mathrm{inc}}} \sum_{\substack{m'=0 \\ m-m' \\ \text{odd}}}^{n'} b_{n'm'}^{\mathrm{inc}} \left( j_{n'}(\kappa r_0) + \frac{\mathrm{d}j_{n'}(\kappa r_0)}{\mathrm{d}\kappa r_0} \right) < Y_{n'm'}^{(\mathrm{e})}, Y_{nm}^{(\mathrm{o})} >_1 \right. + 2 \sum_{\substack{n'=0 \\ n-n' \\ \text{odd}}}^{n^{\mathrm{sca}}} \sum_{\substack{m'=0 \\ m-m' \\ \text{odd}}}^{n'} b_{n'm'}^{\mathrm{sca}} \left( h_{n'}^{(2)}(\kappa r_0) + \frac{\mathrm{d}h_{n'}^{(2)}(\kappa r_0)}{\mathrm{d}\kappa r_0} \right) < Y_{n'm'}^{(\mathrm{e})}, \left. Y_{nm}^{(\mathrm{o})} >_1 \right\} \quad (n = 1,2,\dots,n^{\mathrm{III}}; m = 1,2,\dots,n). \tag{45}$$

Finally, the far-field in domain II is defined by

$$\psi_{\mathrm{h},\infty}^{\mathrm{II}}(r,\vartheta,\varphi) = \sum_{n=0}^{n^{\mathrm{sca}}}\sum_{m=0}^{n} j^{n+1} b_{nm}^{\mathrm{II}}\, Y_{nm}^{(\mathrm{e})}(\vartheta,\varphi). \tag{46}$$

## 5 Numerical Evaluation

### 5.1 Convergence

Since the maximum orders of the multipole expansions and thus the dimensions of the systems of linear equations involved in the solutions basically tend to infinity, the investigation of their convergence properties is of vital interest. Moreover, as the expansion in the inner domain III involves sharp geometrical singularities, it is not a-priori clear that we obtain a converging multipole expansion which is not explicitly including that singularity, at all. To investigate this exemplarily, we consider the geometry in Fig. 3 and the solution for a plane wave incident on an aperture in a plane with an acoustically soft boundary condition. The multipole amplitudes for a plane wave are derived in Appendix B. First, as seen from Eq. (33) the highest degree of the scattered fields $n^{\mathrm{sca}}$ in domains I and II is identical to the highest degree $N = n^{\mathrm{III}}$ of the multipole expansion in the inner domain III. In domain III we have an expansion with spherical Bessel functions, and for a "normal" problem (smooth scatterer) with an electric radius $kr_0$ of the minimum enclosing sphere,

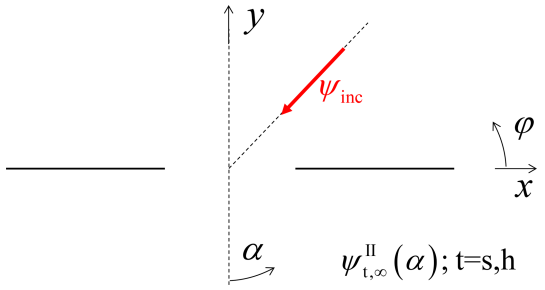


**Figure 3.** Geometry considered for the evaluation of the far-field scattered by the circular aperture.

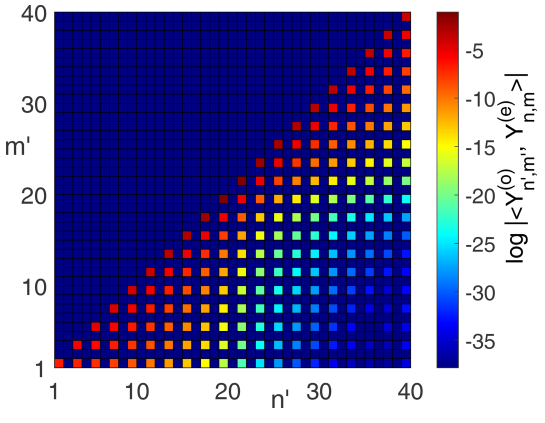


**Figure 4.** Absolute value of the coupling integral (Eq. 24) for a fixed $n = 20, m = 10$ as a function of $n', m'$.

for a reasonable accuracy we would expect a highest relevant degree of about $N \approx kr_0 + 6$, leading to about $N = 12$ for $r_0 = 1\lambda$, see Chew et al. (1998).

Second, for the coupling from the incident field multipole modes to the inner domain III the behaviour of the coupling integrals Eq. (24) is important. Exemplarily, Fig. 4 indicates that the maximum coupling is obtained for same orders, i.e., if $n^{\mathrm{III}} \approx n^{\mathrm{inc}}$ in this context. In other words, to obtain the correct right-hand side amplitudes in Eq. (32), we must choose $n^{\mathrm{inc}}$ sufficiently larger than $N = n^{\mathrm{sca}}$.

Taking this into account we have computed and shown in Fig. 5 the far field for a plane wave scattered by an aperture with radius $r_0 = 1\lambda$ for different maximum orders of $N$. $n^{\mathrm{inc}}$ has been chosen as 40, which turned out to be a sufficiently large number for the cases considered in the following.

As can be observed, a maximum order of $N = 30$ turns out to yield convergent results. Note that this also exemplarily shows that this problem is solvable – on the cost of a significantly higher number of multipoles needed to represent the far field in domain II, as compared to a problem with a smooth scattering object of the same size.

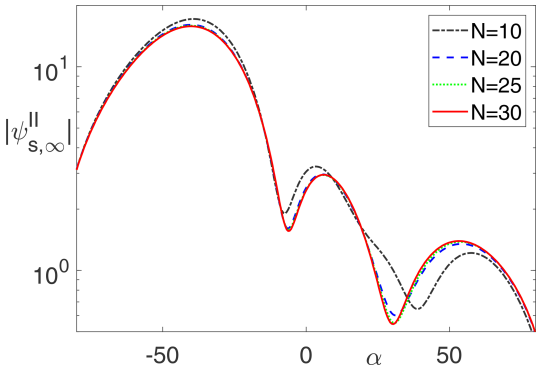


**Figure 5.** Scattered far field for a plane wave illuminating a circular aperture in an acoustically soft plane for different values of the maximum degree $N = n^{\mathrm{sca}}$ of the spherical-multipole expansion of the scattered field. Angle of incidence $\phi^{\mathrm{inc}} = 45°$; Radius of the aperture: $r_0 = 1\lambda$; The maximum degree of the spherical-multipole expansion of the incident field has been chosen to $n^{\mathrm{inc}} = 40$; $\alpha$ is defined in Fig. 3.

### 5.2 Validation

In order to validate the results, Figs. 6 and 7 show the far fields in domain II for a plane wave symmetrically (with respect to the $y$ axis and to the aperture) incident on a circular aperture of different radii. The outcomes of the present method are compared to those ones obtained for the case of a plane wave symmetrically incident on a disc of same size. By applying Babinet's principle we have to compare the results of a plane wave incident on an circular aperture in an acoustically soft plane to those ones of the same plane wave but incident on an acoustically hard disc of same size (and vice versa). The latter results have been obtained by means of exactly solving the Helmholtz equation in oblate ellipsoidal coordinates where the disc is a coordinate surface. These results are taken from Bowman et al. (1988).

Note that for both of the figures no further normalization (except of dropping the spherical-wave term) of the amplitude has been applied. While we observe a relatively good agreement for aperture (disc) radii $kr_0 = 1$ and $kr_0 = 3$, the differences increase for $kr_0 = 5$ particularly in the near of the symmetry axis ($\alpha = 0$). Because of the symmetry of the incident plane wave we expect a zero tangent of the curve for $\alpha = 0$, which quite obviously is not the case for the result taken from Bowman et al. (1988) rendering them as inaccurate.

### 5.3 Numerical results for an aperture in an acoustically soft screen

Figure 8 shows the real part of the phasor of the near field $\psi_s$. A plane wave is incident from $\varphi^{\mathrm{inc}} = 45°$ on the aperture of radius $r_0 = 1\lambda$ in an acoustically soft screen. Note that this is identical to a snapshot of the time-domain field at $t = 0$. For $y > 0$ we observe the typical interference pattern produced

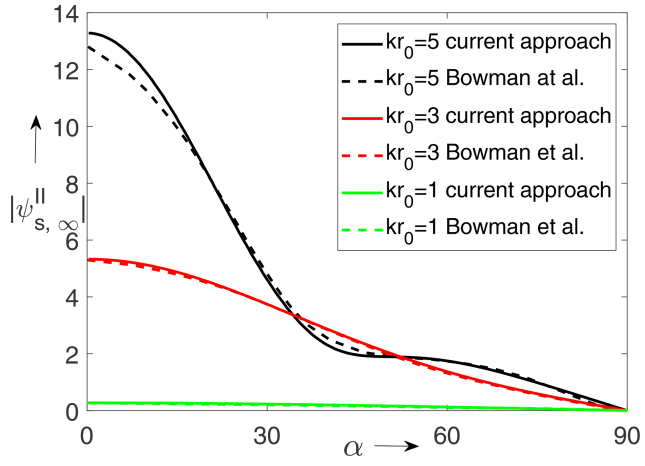


**Figure 6.** Plane wave symmetrically incident on a circular aperture of different radii in an acoustically soft screen. Present approach (solid line) and results taken from Bowman et al. (1988) for an acoustically hard disc; $\alpha$ is defined in Fig. 3.

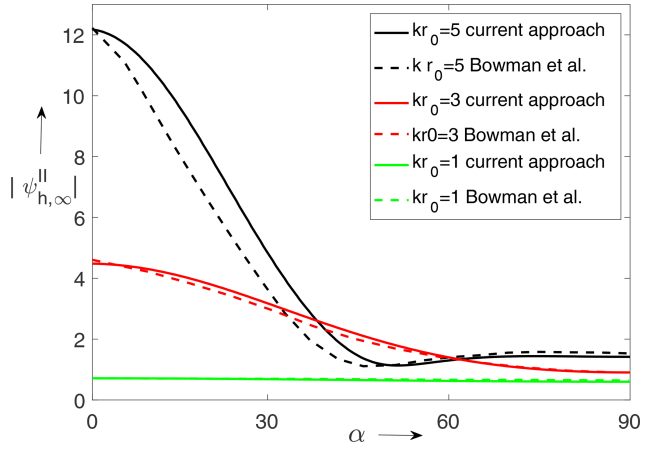


**Figure 7.** Plane wave symmetrically incident on a circular aperture of different radii in an acoustically hard screen. Present approach (solid line) and results taken from Bowman et al. (1988) for an acoustically soft disc; $\alpha$ is defined in Fig. 3.

by the superposition of the incident and the reflected field, while for $y < 0$ the typical diffraction pattern of an aperture can be observed. The field and its derivative is continuous for $r = r_0$ which also proves the convergence and consistency of the method for the numbers of multipoles chosen, and the correctness of the numerical implementation.

In Fig. 9 we see the absolute amplitude of the field in the aperture for $y = z = 0, -1\lambda < x < 1\lambda$) for different values of $n^{\mathrm{III}}$. Apart from the edge at $r = r_0$ the field converges well with a finite number of multipole amplitudes. At $r = r_0$ the field converges very slowly against zero which is expected as the field should be zero at the sharp rim only whereas it has to be non-zero and continuous for all other values.

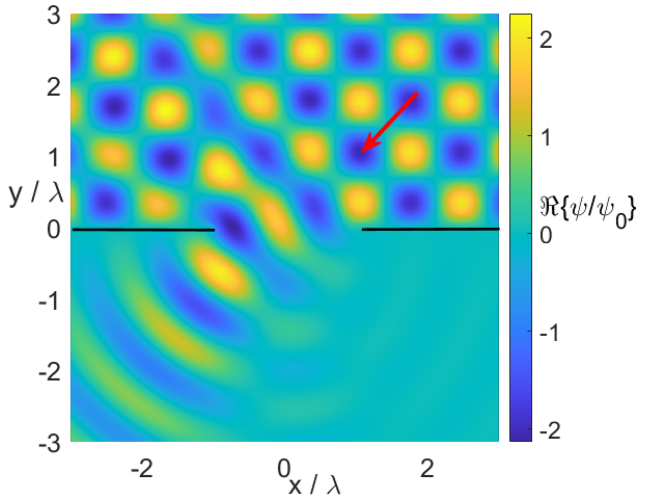


**Figure 8.** Plane wave incident on a circular aperture in an acoustically soft screen. Real part of the near field $\psi_s(\boldsymbol{r})$. Radius of the aperture: $r_0 = 1\lambda$; $\phi^{\mathrm{inc}} = 45°$; $n^{\mathrm{sc}} = 30$; $n^{\mathrm{inc}} = 40$.

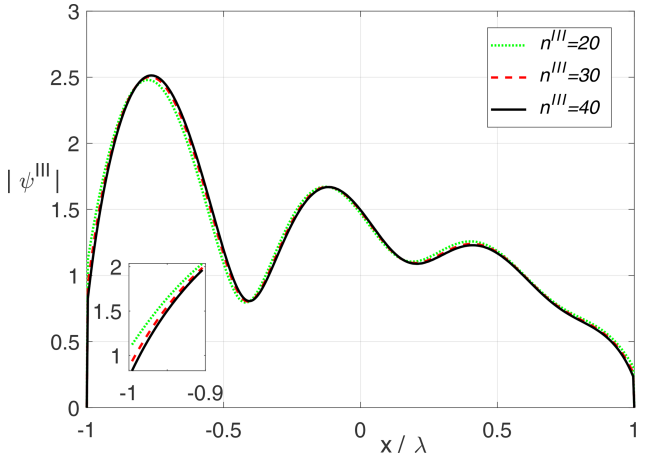


**Figure 9.** Absolute value of $\psi_s^{\mathrm{III}}(\boldsymbol{r})$ in the aperture for $(y = z = 0)$ as a function of $x$ for different value of $n^{\mathrm{III}}$. Plane wave incident $(\varphi^{\mathrm{inc}} = 45°)$ on a circular aperture with radius $r_0 = 1\lambda$ in an acoustically soft screen. $n^{\mathrm{inc}} = 50$.

Figure 10 shows the near-field for the same geometry as in Fig. 8 but with an incident uniform Complex-Source Beam (uniform CSB). The derivation of the corresponding multipole amplitudes is attached in Appendix C. Since the waist of the uniform CSB has been located almost in the aperture and the beam width at the waist is $w_0/\lambda = 2\sqrt{b/\lambda(1/\pi)} \approx 3.57$, the interaction between the uniform CSB in its waist and the aperture are expected to be quite similar as for a corresponding incident plane wave. Thus it is not surprising that the scattered far fields for both, an incident plane wave and an incident uniform CSB are essentially the same as shown in Fig. 11. Further note that the far-field results are much faster converging than the field at or nearby the rim ($r = r_0$; $y = 0$), see Fig. 9. The results also support the idea, that for the inves-

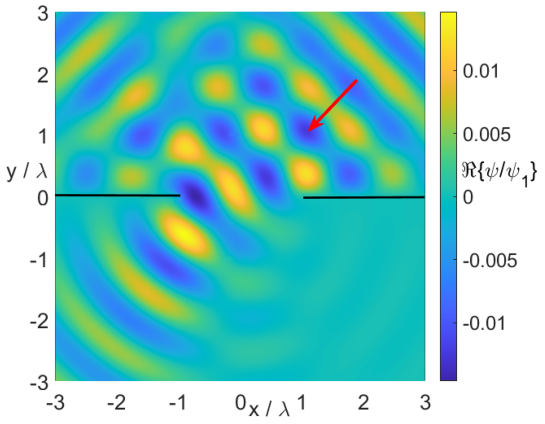


**Figure 10.** Uniform CSB incident on a circular aperture in an acoustically soft screen. Real part of the near field $\psi_s(\boldsymbol{r})$. Radius of the aperture: $r_0 = 1\lambda$. Coordinates of the waist: $r_w = 0.01\lambda$; $\vartheta_w = 90°$; $\varphi_w = 45°$; Rayleigh length: $b = 10\lambda$; $n^{sc} = 30$; $n^{inc} = 40$.

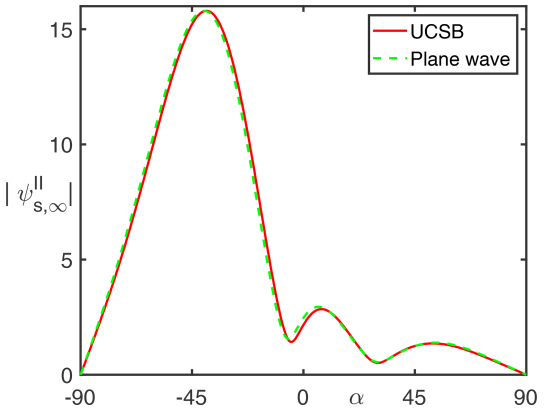


**Figure 11.** Plane wave and uniform CSB incident on a circular aperture in an acoustically soft screen: Comparison of the scattered far fields $\psi^{II}_{s,\infty}$. $r_0 = 1\lambda$; $\phi^{inc} = 45°$; Coordinates of the waist: $r_w = 0.01\lambda$; $\vartheta_w = 90°$; $\varphi_w = 45°$; Rayleigh length: $b = 10\lambda$; $n^{sc} = 30$; $n^{inc} = 40$; $\alpha$ is defined in Fig. 3.

tigation of a local phenomenon of infinite semi-infinite structures (e.g., the tip of a semi-infinite cone) we may use a uniform CSB instead of a plane wave which leads to drastically reduced convergence problems of multipole expansions.

### 5.4 Numerical results for an aperture in an acoustically hard screen

Figure 12 shows the real part of the field phasor for a plane wave incident on an aperture (radius $r_0 = 1\lambda$) in an acoustically hard plane. Figure 13 represents the corresponding absolute values of the normal field derivative in the aperture. We clearly observe an (expected) field singularity at the rim ($r = r_0$) which is more and more developed with an increasing number of multipoles $n^{III}$. In Fig. 14 we see the corresponding near-field for an incident uniform CSB, while finally Fig. 15 shows that the scattered far fields for both, an incident plane wave and an incident uniform CSB.

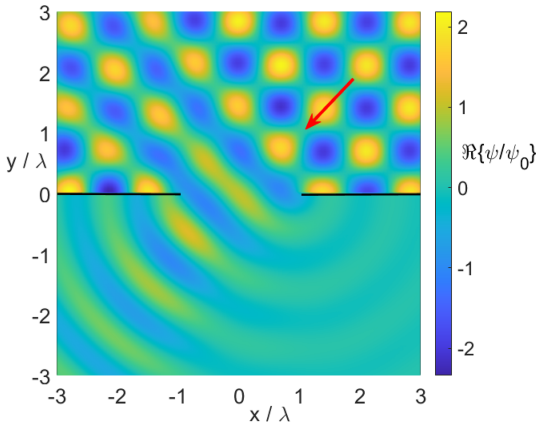


**Figure 12.** Plane wave incident on a circular aperture in an acoustically hard screen; $\varphi^{inc} = 45°$. Real part of the near field $\psi_h(\boldsymbol{r})$. $r_0 = 1\lambda$; $n^{sc} = 30$; $n^{inc} = 40$.

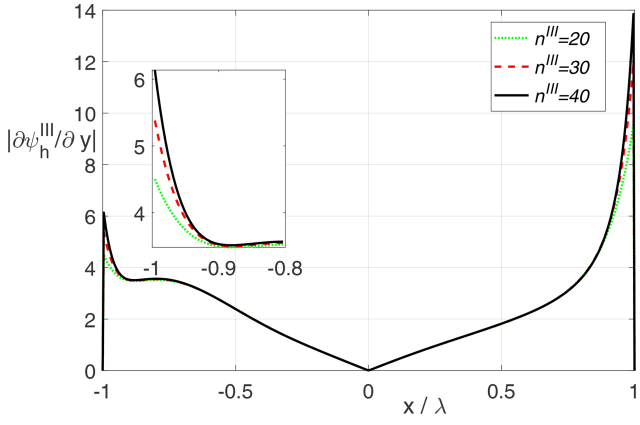


**Figure 13.** Plane wave incident on a circular aperture in an acoustically hard screen: Absolute value of the derivative $\partial\psi_h^{III}/\partial y$ in the aperture ($y = z = 0$) as a function of $x$ for different values of $n^{III}$. $\varphi^{inc} = 45°$); $r_0 = 1\lambda$; $n^{inc} = 50$.

## 6 Conclusions and Outlook

It has been shown that the classical canonical problem for an aperture in an acoustically soft or hard infinite plane screen can be solved analytically by means of a three-domain problem and suitable spherical-multipole expansions in each of the domains. All integrals which occur in the context of solving the boundary-value problems can be solved analytically. Moreover, the solution is performed by means of ordinary spherical coordinates and corresponding elementary solutions of the Helmholtz equation, i.e., spherical Bessel and Hankel functions and surface spherical harmonics with integer degrees and orders. Solutions of the Helmholtz equation in spheroidal wave functions and their sometimes as "diffi-

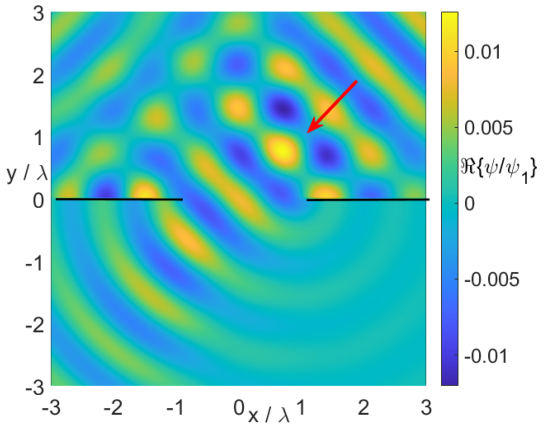


**Figure 14.** Uniform CSB incident on a circular aperture in an acoustically hard screen. Real part of the near field $\psi_s(\boldsymbol{r})$. $r_0 = 1\lambda$; $n^{\mathrm{sc}} = 30$; $n^{\mathrm{inc}} = 40$. Coordinates of the waist: $r_{\mathrm{w}} = 0.01\lambda$; $\vartheta_{\mathrm{w}} = 90°$; $\varphi_{\mathrm{w}} = 45°$; Rayleigh length: $b = 10\lambda$.

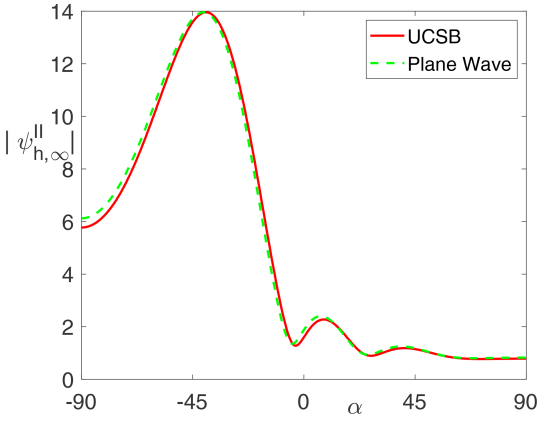


**Figure 15.** Plane wave and uniform CSB incident on a circular aperture in an acoustically hard screen: Scattered far field $\psi^{\mathrm{II}}_{\mathrm{s},\infty}$. $r_0 = 1\lambda$; $\varphi^{\mathrm{inc}} = 45°$); Coordinates of the waist: $r_{\mathrm{w}} = 0.01\lambda$; $\vartheta_{\mathrm{w}} = 90°$; $\varphi_{\mathrm{w}} = 45°$; Rayleigh length: $b = 10\lambda$;$n^{\mathrm{sc}} = 30$; $n^{\mathrm{inc}} = 40$; $\alpha$ is defined in Fig. 3.

cult" reported numerical calculation (Zeppenfeld, 2009) are completely avoided. The resulting series solutions turn out to deliver correct results with a stable but comparatively slow convergence. The latter is mainly due to the fact that singular field values we expect at the rim of the aperture are not explicitly expressed by the series expansions but achieved for an infinite number of multipoles only. In contrast, for other observation points particularly in the far-field a limited number of multipoles is sufficient for any reasonable accuracy. Future research includes the further investigation of the outcome that for a field representation outside of the rim only a certain part of the modal expansion of the singularity is relevant. Moreover, future research includes the solution and analysis of the corresponding electromagnetic problem.

## Appendix A: Analytical evaluation of the integral on a product of two Ferrers functions with different orders and degrees

The derivation follows that one given by Wong (1998). Since the result presented here slightly differs from the one given in Wong (1998) and some of the formulaes can not be found in the standard literature, the basic steps of the derivation are included in this work.

To analytically evaluate the integral

$$I_{n,m;n',m'} = \int_{-1}^{+1} P_n^m(x) P_{n'}^{m'}(x) \mathrm{d}x \tag{A1}$$

we start from the representations of the associated Legendre function "on the cut", also known as Ferrers' function, valid for integral values of $n$ and $m$ for a real-valued argument $-1 \le x \le +1$

$$\begin{aligned} P_n^m(x) &= (-1)^{m+n} \frac{\left(1-x^2\right)^{m/2}}{2^n n!} \frac{\mathrm{d}^{m+n}}{\mathrm{d}x^{m+n}} \left(1-x^2\right)^n \\ &= \sum_{p=0}^{p_{\max}} a_{n,m}^p \left(1-x^2\right)^{\frac{m+1}{2}p} x^{n-m-2p} \end{aligned} \tag{A2}$$

where

$$a_{n,m}^p = \frac{(-1)^{m+p}(n+m)!}{2^{m+2p}(m+p)!p!(n-m-2p)!} \tag{A3}$$

$$p_{\max} = \lfloor \frac{n-m}{2} \rfloor. \tag{A4}$$

In Eq. (A4), $\lfloor x \rfloor$ means the highest integer not larger than $x$. Inserting Eq. (A2) into Eq. (A1) yields

$$\begin{aligned} I_{n,m;n',m'} &= \sum_{p=0}^{p_{\max}} a_{n,m}^p \sum_{p'=0}^{p'_{\max}} a_{n',m'}^{p'} \int_{-1}^{+1} (1-x^2)^{\frac{m+2p+m'+2p'}{2}} \\ &\quad x^{n+n'-m-m'-2p-2p'} \mathrm{d}x \\ &= \begin{cases} 2\sum_{p=0}^{p_{\max}} a_{n,m}^p \sum_{p'=0}^{p'_{\max}} a_{n',m'}^{p'} \int_0^{+1} (1-x^2)^{\frac{m+2p+m'+2p'}{2}} \\ x^{n+n'-m-m'-2p-2p'} \mathrm{d}x & \text{if } n+n'-m-m' \text{ even} \\ 0 & \text{else.} \end{cases} \end{aligned} \tag{A5}$$

A comparison of the integral in Eq. (A5) with the definition of the Beta-function

$$B(a,b) = \int_0^{+1} t^{a-1}(1-t^2)^{b-1} \mathrm{d}t = \frac{\Gamma(a)\Gamma(b)}{\Gamma(a+b)} \tag{A6}$$

leads after a suitable substitution $t = x^2$ to the final result

$$I_{n,m;n',m'} = \begin{cases} \sum_{p=0}^{p_{\max}} a_{n,m}^p \sum_{p'=0}^{p'_{\max}} a_{n',m'}^{p'} \\ \frac{\Gamma\left[\frac{1}{2}(n+n'-m-m'-2p-2p'+1)\right]\Gamma\left[\frac{1}{2}(m+m'+2p+2p'+2)\right]}{\Gamma\left[\frac{1}{2}(n+n'+3)\right]} \\ \qquad \text{if } n+n'-m-m' \text{ even} \\ 0 \qquad \text{else.} \end{cases} \tag{A7}$$

## Appendix B: Spherical-multipole expansion of an arbitrary plane wave in the presence of a plane

In order to describe an arbitrarily incident plane wave propagating in the direction $-\hat{n}$ in the presence of an acoustically soft or hard plane by means of a spherical-multipole expansion, we are looking for the multipole amplitudes $a_{nm}^{\mathrm{inc}}$ and $b_{nm}^{\mathrm{inc}}$ which satisfy the following relation

$$\psi^{\mathrm{inc}} = A_0 e^{j\kappa\hat{n}\cdot\boldsymbol{r}} = \sum_{n=0}^{\infty}\sum_{m=0}^{n} j_n(\kappa r)\Big[a_{nm}^{\mathrm{inc}} Y_{nm}^{(\mathrm{o})}(\vartheta,\varphi) + b_{nm}^{\mathrm{inc}} Y_{nm}^{(\mathrm{e})}(\vartheta,\varphi)\Big] \tag{B1}$$

To this end, we start from the comparison of the closed and bilinear forms of the free-space Green's function in case of $r < r'$

$$\frac{1}{4\pi}\frac{e^{-j\kappa|\boldsymbol{r}-\boldsymbol{r}'|}}{|\boldsymbol{r}-\boldsymbol{r}'|} = -j\kappa\sum_{n=0}^{\infty}\sum_{m=0}^{n} j_n(\kappa r)h_n^{(2)}(\kappa r') \Big[Y_{nm}^{(\mathrm{o})}(\vartheta,\varphi)Y_{nm}^{(\mathrm{o})}(\vartheta',\varphi') + Y_{nm}^{(\mathrm{e})}(\vartheta,\varphi)Y_{nm}^{(\mathrm{e})}(\vartheta',\varphi')\Big] \tag{B2}$$

For $\kappa r' \to \infty$, a Taylor expansion of the left-hand side in Eq. (B2) and the asymptotic expression of the spherical Hankel function of the second kind [see Eq. (35)] yields

$$\frac{1}{4\pi}e^{-j\kappa\hat{r}'\cdot\boldsymbol{r}}\frac{e^{-j\kappa r'}}{r'} = -j\kappa\sum_{n=0}^{\infty}\sum_{m=0}^{n} j_n(\kappa r)(j)^{n+1}\frac{e^{-j\kappa r'}}{r'} \Big[Y_{nm}^{(\mathrm{o})}(\vartheta,\varphi)Y_{nm}^{(\mathrm{o})}(\vartheta',\varphi') + Y_{nm}^{(\mathrm{e})}(\vartheta,\varphi)Y_{nm}^{(\mathrm{e})}(\vartheta',\varphi')\Big] \tag{B3}$$

A comparison of the orthogonal expansions Eq. (B1) and Eq. (B3) leads to the desired result

$$a_{nm}^{\mathrm{inc}} = A_0 4\pi\, j^n Y_{nm}^{(\mathrm{o})}(\vartheta',\varphi') \tag{B4}$$

$$b_{nm}^{\mathrm{inc}} = A_0 4\pi\, j^n Y_{nm}^{(\mathrm{e})}(\vartheta',\varphi') \tag{B5}$$

with $\hat{n} = \hat{r}'$. For the incident plane wave used in this paper we have to set $b_{n,m}^{\mathrm{inc}} \equiv 0$ ($a_{n,m}^{\mathrm{inc}} \equiv 0$) for the aperture in a acoustically soft (hard) infinite plane.

## Appendix C: Spherical-multipole expansion of a uniform complex-source beam in the presence of a plane

A complex-source beam is obtained by simply extending the real-valued coordinate $\boldsymbol{r}'$ where a point source is located to the complex domain

$$\boldsymbol{r}_c = \boldsymbol{r}' - j\boldsymbol{r}_b \tag{C1}$$

As has been shown, the outwardly travelling field of the point source then turns into a complex-source beam which starts at $\boldsymbol{r}'$ and is travelling in the direction of $\boldsymbol{r}_b$. Nearby the axis of propagation the CSB approximates half of a Gaussian beam with a waist centered at $\boldsymbol{r}'$ and a Rayleigh length of $r_b$. Similarly, an approach for an inwardly travelling field of a point sink leads to the other half of the Gaussian beam. Consequently, a superposition of outwardly and inwardly travelling CSBs then approximates a complete Gaussian beam. In contrast to a single CSB the superposition is regular also in the waist and in this paper referred to as a uniform CSB. Note that a uniform CSB contains also other field parts travelling in the opposite direction which however are usually of negligibly small amplitude.

In closed form a uniform CSB can be expressed as

$$\psi^{\mathrm{inc}}(\boldsymbol{r}) = B_0\left[\frac{e^{j\kappa|\boldsymbol{r}-\boldsymbol{r}_c|}}{\kappa|\boldsymbol{r}-\boldsymbol{r}_c|} - \frac{e^{-j\kappa|\boldsymbol{r}-\boldsymbol{r}_c|}}{\kappa|\boldsymbol{r}-\boldsymbol{r}_c|}\right] = \frac{B_0}{2j}\frac{\sin(\kappa|\boldsymbol{r}-\boldsymbol{r}_c|)}{\kappa|\boldsymbol{r}-\boldsymbol{r}_c|} \tag{C2}$$

where the amplitude $B_0$ may be normalized to the constant $e^{\kappa r_b}$ to avoid huge numbers in the field amplitude. Using the identity Eq. (B2) the corresponding bilinear form reads

$$\psi^{\mathrm{inc}}(\boldsymbol{r}) = -8\pi j B_0\sum_{n=0}^{\infty}\sum_{m=0}^{n} j_n(\kappa r)j_n(\kappa r_c) \Big[Y_{nm}^{(\mathrm{o})}(\vartheta,\varphi)Y_{nm}^{(\mathrm{o})}(\vartheta',\varphi') + Y_{nm}^{(\mathrm{e})}(\vartheta,\varphi)Y_{nm}^{(\mathrm{e})}(\vartheta',\varphi')\Big]. \tag{C3}$$

Thus, the multipole amplitudes of the spherical-multipole expansion

$$\psi^{\mathrm{inc}} = \sum_{n=0}^{\infty}\sum_{m=0}^{n} j_n(\kappa r)\Big[a_{nm}^{\mathrm{inc}} Y_{nm}^{(\mathrm{o})}(\vartheta,\varphi) + b_{nm}^{\mathrm{inc}} Y_{nm}^{(\mathrm{e})}(\vartheta,\varphi)\Big] \tag{C4}$$

are given by

$$a_{nm}^{\mathrm{inc}} = -B_0 j 8\pi\, j_n(\kappa r_c)Y_{nm}^{(\mathrm{o})}(\vartheta',\varphi') \tag{C5}$$

$$b_{nm}^{\mathrm{inc}} = -B_0 j 8\pi\, j_n(\kappa r_c)Y_{nm}^{(\mathrm{e})}(\vartheta',\varphi') \tag{C6}$$

Note that for a uniform CSB there is no need for a case distinction $r \gtrless r'$ as it usually is necessary for a bilinear field expansions with real-valued source coordinates. Again, for the incident uniform CSB used in this paper we have to set $b_{n,m}^{\mathrm{inc}} \equiv 0$ ($a_{n,m}^{\mathrm{inc}} \equiv 0$) for the aperture in a acoustically soft (hard) infinite plane.

*Code availability.* All FORTRAN codes used in this work have been written by the author. Since they will be used for further publications, they are not available. Standard parts of the code (e.g., the solution of a system of linear equations) are based on software from the NAG-Library (https://nag.com/nag-library/, NAG, 2025). The graphs have been produced using MATLAB (https://mathworks.com/, MathWorks, 2025).

*Data availability.* The data represented in the numerical results in this paper are available from the author upon request.

*Competing interests.* The author has declared that there are no competing interests.

*Disclaimer.* Publisher's note: Copernicus Publications remains neutral with regard to jurisdictional claims made in the text, published maps, institutional affiliations, or any other geographical representation in this paper. While Copernicus Publications makes every effort to include appropriate place names, the final responsibility lies with the authors.

*Special issue statement.* This article is part of the special issue "Kleinheubacher Berichte 2024". It is a result of the Kleinheubacher Tagung 2024, Miltenberg, Germany, 24–26 September 2024.

*Review statement.* This paper was edited by Simon Adrian and reviewed by two anonymous referees.

## References

Andrejewski, W.: Die Beugung elektromagnetischer Wellen an der leitenden Kreisscheibe und an der kreisformigen Offnung im leitenden ebenen Schirm, Z. Angew. Physik, 5, 178–186, 1953.

Bethe, H. A.: Theory of Diffraction by Small Holes, Phys. Rev., 66, 163–182, 1944.

Bouwkamp, C. J.: Theoretische En Numerieke Behandeling van de Buiging Door Zen Ronde Opening, PhD theses, University of Groningen(Holland), https://research.rug.nl/nl/publications/theoretische-en-numerieke-behandeling-van-de-buiging-door-een-ron (last access: 10 March 2025), 1941.

Bouwkamp, C. J.: A Note on Singularities Occuring at Sharp Edges in Electromagnetic Diffraction Theory, Physica VII, 467–477, https://doi.org/10.1016/S0031-8914(46)80061-2, 1946.

Bowman, J. J., Senior, T. B. A., and Uslenghi, P. L. E.: Electromagnetic and Acoustic Scattering by Simple Shapes, Chap. 14: The Disc, Revised Edition, Taylor & Francis Inc., ISBN 978-0891168850, 1988.

Braunbek, W.: Zur Beugung an der Kreisscheibe, Z. Phys., 127, 405–415, 1950.

Chew, W. C., Jin, J.-M., Michielssen, E., and Song, J. (Eds.): Fast and Efficient Algorithms in Computational Electromagnetics, Boston, Artech House, p. 52f., ISBN 978-1580531528, 2000.

De Hoop, A. T.: On The Scalar Diffraction by a Circular Aperture in an Infinite Plane Screen, Appl. Sci. Res. B-Elec., 4, 151–160, 1954.

Dunster, T. M.: Legendre and Related Functions, in: Digital Library of Mathematical Funcions, Chap. 14, https://dlmf.nist.gov/14, last access 26 Februray 2025.

Keller, J. B.: Diffraction by an Aperture, J. Appl. Phys., 28, 426–444, https://doi.org/10.1063/1.1722767 , 1957.

Keller, J. B., Lewis, R. M., and Seckler, B. D.: Diffraction by an Aperture II, J. Appl. Phys., 28, 570–579, https://doi.org/10.1063/1.1722805, 1957.

Klinkenbusch, L.: Scattering and diffraction of a uniform complex-source beam by a slit in a perfectly conducting plane screen, Adv. Radio Sci., 18, 43–52, https://doi.org/10.5194/ars-18-43-2020, 2020.

Klinkenbusch, L.: Diffraction by a Circular Aperture: A New Spherical-Multipole Approach, Proc. of the 2024 IEEE International Symposium on Antennas and Propagation and INC/USNC-URSI Radio Science Meeting, Florence (Italy), 14–19 July 2024, https://doi.org/10.1109/AP-S/INC-USNC-URSI52054.2024.10686328, 2024a.

Klinkenbusch, L.: Diffraction by a Circular Aperture in an Acoustically Hard Plane, Proc. of the 2024 Kleinheubach Conference, Miltenberg (Germany), 24–26 September 2024, ISBN 78-3-948571-14-6, https://magentacloud.de/s/ND9wRq3qKSHyNrR (last access: 10 March 2025), 2024b.

Kristensson, G. and Waterman, P. C.: The T-Matrix for Acoustic and Electromagnetic Scattering by Circular Disks, J. Acoust. Soc. Am., 72, 1612–1625, 1982.

Kuryliak, D. and Lysechko, V.: Diffraction of the Sound Wave from a Soft Disc, Proc. of the 2015 XXth International Seminar/Workshop on Direct and Inverse Problems of Electromagnetic and Acoustic Wave Theory (DIPED), 197–182, https://doi.org/10.1109/DIPED.2015.7324293, 2015.

Levine, H. and Schwinger, J.: On the Theory of Diffraction by an Aperture in an Infinite Plane Screen. I, Phys. Rev., 74, 958–974, 1948a.

Levine, H. and Schwinger, J.: On the Theory of Diffraction by an Aperture in an Infinite Plane Screen. II, Phys. Rev., 74, 1423–1432, 1948b.

MathWorks: MATLAB for Artificial Intelligence, Mathworks [code], https://mathworks.com/, last access: 10 March 2025.

Meixner, J.: Strenge Theorie der Beugung elektromagnetischer Wellen an der vollkommen leitenden Kreisscheibe, Z. Naturforsch., 3, 506–518, 1948.

NAG: NAG Library, NAG [code], https://nag.com/nag-library/, last access: 10 March 2025.

Rayleigh, F. R. S.: On the incidence of aerial and electric waves upon small obstacles in the form of ellipsoids or elliptic cylinders, and on the passage of electric waves through a circular aperture in a conducting screen, The London, Edinburgh, and Dublin Philosophical Magazine and Journal of Science, 44, 28–52, 1897.

Sommerfeld, A.: Vorlesungen über Theoretische Physik, Band VI: Differentialgeichungen, 2nd edn., 28–31, Wiesbaden: Dieterisch'sche Verlagsbuchhandlung, 1947.

Wong, B. R.: On the Overlap Integral of Associated Legendre Polynomials, J. Phys. A-Math. Gen., 31, 1101–1103, 1998.

Zeppenfeld, K.: Solutions to Maxwell's equations using spheroidal coordinates, New J. Phys., 11, 073007, https://doi.org/10.1088/1367-2630/11/7/073007, 2009.